Ceramics International 50 (2024) 3912–3920

Contents lists available at ScienceDirect

Ceramics International

journal homepage: www.elsevier.com/locate/ceramint

Effects of ion occupancy and polarizability on the crystal structure and microwave dielectric properties of CaEuCO$_4$ (C=Ga, Al) ceramics

Yang Yang [a], Weishuang Fang [a], Ning Zhang [a], Huaicheng Xiang [a,b,*], Ying Tang [a,b], Jie Li [a], Liang Fang [a]

[a] Guangxi Universities Key Laboratory of Non-Ferrous Metal Oxide Electronic Functional Materials and Devices, Guangxi Key Laboratory of Optical and Electronic Materials and Devices, College of Materials Science and Engineering, Guilin University of Technology, Guilin, 541004, China
[b] Key Laboratory of Low-Dimensional Structural Physics and Application, Education Department of Guangxi Zhuang Autonomous Region, College of Physics and Electronic Information Engineering, Guilin University of Technology, Guilin, 541004, China

ARTICLE INFO

Handling Editor: Dr P. Vincenzini

Keywords:
Olivine and K_2NiF_4 structure
Microwave dielectric properties
Bond valance
Covalence

ABSTRACT

CaEuCO$_4$ (C=Ga, Al) microwave dielectric ceramics were produced through a solid-state reaction. Orthorhombic olivine CaEuGaO$_4$ (*pnma*) exhibits a lower permittivity ($\varepsilon_r = 9.7$), a higher quality factor ($Q \times f = 82{,}049$ GHz), and a larger negative resonant frequency temperature coefficient ($\tau_f = -54.6$ ppm/°C). CaEuAlO$_4$, which has a similar chemical formula, exhibits a perovskite-like structure (*I4/mmm*, K_2NiF_4-type), and its microwave dielectric properties are $\varepsilon_r = 18.9$, $Q \times f = 43{,}132$ GHz, and $\tau_f = -1.6$ ppm/°C. The difference in their structures is mainly caused by the properties of the Ga (III) atom. The difference in their dielectric properties can be proved to be affected by the "rattling" effect of Eu^{3+} through the bond valence theory. The relationship between the covalence (f_c) and the bond strength (S) was investigated, and the higher bond strength might be the main reason for the higher $Q \times f$ in CaEuGaO$_4$ ceramic.

1. Introduction

A majority of CaLnGaO$_4$ (Ln = Lanthanides) compounds crystallize in the olivine-type structure in the orthorhombic space group *pnma* [1,2]. The Ga is coordinated tetrahedrally, while the rare earth and Ca occupy octahedron locations. CaLaGaO$_4$ can also crystallize in a K_2NiF_4-type structure, where Ga atoms are octahedrally coordinated, and La and Ca atoms randomly occupy the remaining dodecahedron sites [3,4]. K_2NiF_4-type perovskite-like compounds exhibit a wide variety of technologically essential properties. Most reported results focus on high-temperature superconductivity, ferroelectric, and dielectric properties [5–8]. For instance, the microwave dielectric properties of $ABCO_4$ (A = Ca, Sr; B=La, Nd, Sm, Y; C=Al, Ga) ceramics were characterized by low permittivity ε_r (17.6–18.4), high quality factor $Q \times f$ (55,000–70,000 GHz), and a wide range of resonant frequency temperature coefficient τ_f (−33.5 - +7.1 ppm/°C) [9–16]. As early as 1992, Shannon [16] found that the molecular dielectric polarizability of CaYAlO$_4$, CaNdAlO$_4$, and SrLaAlO$_4$ with tetragonal perovskite-like structure was not consistent with the sum rule of individual ion polarizability, which was caused by the "rattling" or "compressed" state of A and B cations.

As shown in Fig. 1, with the increase of ε_r, the τ_f decreased slightly from −48.1 to −58.4 ppm/°C in olivine CaLnGaO$_4$ (*pnma*), while in K_2NiF_4-type perovskite-like ceramics (*I4/mmm*), the τ_f increased significantly from −33.5 to 7.1 ppm/°C. Although the variation of τ_f in K_2NiF_4-type ceramics is consistent with the dilution mechanism of ion polarizability, the increase of τ_f with ε_r is much larger than that of conventional systems. Colla and Reaney et al. [17,18] studied the link between the tolerance factor (t) and τ_f of perovskite materials. They believed the phase transition caused by the tilt of the oxygen octahedron in the structure was the most important factor affecting τ_f. However, in the system without structural phase transition, the variation of τ_f with ε_r is slight, and the τ_f value does not change abruptly from negative to positive, such as in $RE_3Ga_5O_{12}$ [19], $RE_3Al_5O_{12}$ [20], AGa_2O_4 (A = Zn, Mg) [21–23], and AAl_2O_4 (A = Zn, Mg) [24,25]. Since the structural chemistry of gallium (III) is similar to that of aluminum (III), Ga^{3+} and Al^{3+} are introduced into the C-site of CaEuCO$_4$ ceramics in this work to investigate their structural changes and the effects of the state of cations

* Corresponding author. Guangxi Universities Key Laboratory of Non-Ferrous Metal Oxide Electronic Functional Materials and Devices, Guangxi Key Laboratory of Optical and Electronic Materials and Devices, College of Materials Science and Engineering, Guilin University of Technology, Guilin, 541004, China.
E-mail address: xianghc@glut.edu.cn (H. Xiang).

https://doi.org/10.1016/j.ceramint.2023.11.154
Received 18 September 2023; Received in revised form 1 November 2023; Accepted 13 November 2023
Available online 15 November 2023

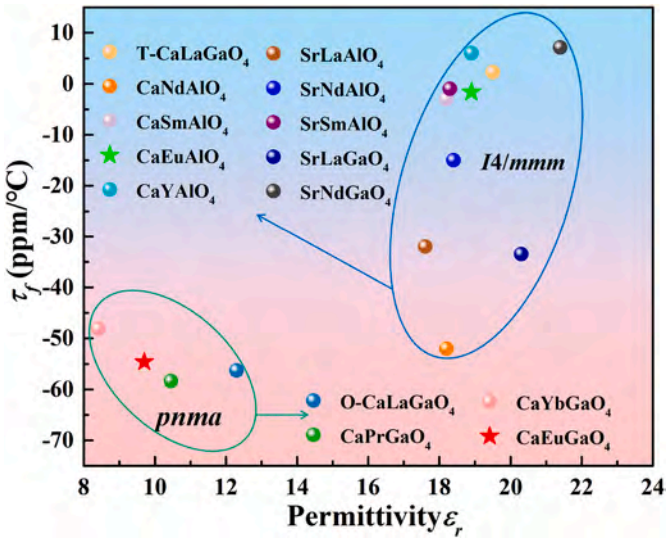

Fig. 1. The relationship between ε_r and τ_f in olivine-type (*pnma*) and K_2NiF_4-type (*I4/mmm*) Ca*Ln*GaO_4 ceramics.

at each site on the microwave dielectric properties.

2. Experimental procedure

$CaEuGaO_4$ and $CaEuAlO_4$ materials were prepared by solid phase synthesis (Fig. 2). Eu_2O_3, $CaCO_3$, Ga_2O_3, and Al_2O_3 powders (99.99 %, Aladdin) were mixed in a stoichiometric ratio in absolute ethanol (>99.7 %, XiLong Scientific). These slurries were dried at 120 °C to obtain solid powders and calcined at 1100 °C for 6 h. The calcined powders were ball-milled for 6 h, and 5 wt% polyvinyl alcohol (PVA) was added as a binder to press into cylinders (diameter 10, height 5) and finally sintered at 1180–1240 °C and 1380–1440 °C, respectively.

Powder X-ray diffraction (PANalytical, X'Pert Pro) was used for phase detection in the range of 10–120° at room temperature. The obtained powder diffraction patterns were subjected to Rietveld refinement with FULLPROF software. Archimedes' technique was used to calculate the bulk density of the samples. Thermally etched surfaces were examined using a field emission scanning electronic microscope (FESEM, Hitachi S-4800) to acquire bulk microstructures. The temperature-dependent thermal expansion rates (25–275 °C) were tested by Simultaneous Thermal Analyzer (STA 449 F, NETZSCH, Germany). The resonant frequency (f), ε_r, and $Q \times f$ were measured using a network analyzer (N5230A, Agilent) using the TE_{011} technique [26]. Temperature coefficients of f and ε_r were calculated as follows:

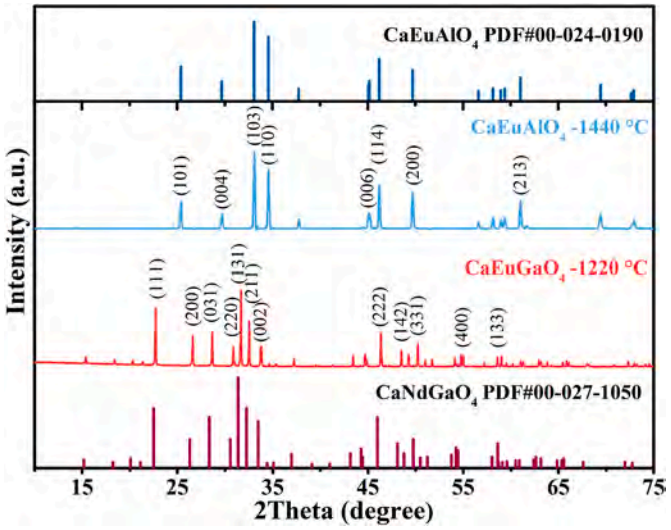

Fig. 3. XRD patterns of $CaEuGaO_4$ and $CaEuAlO_4$ ceramics.

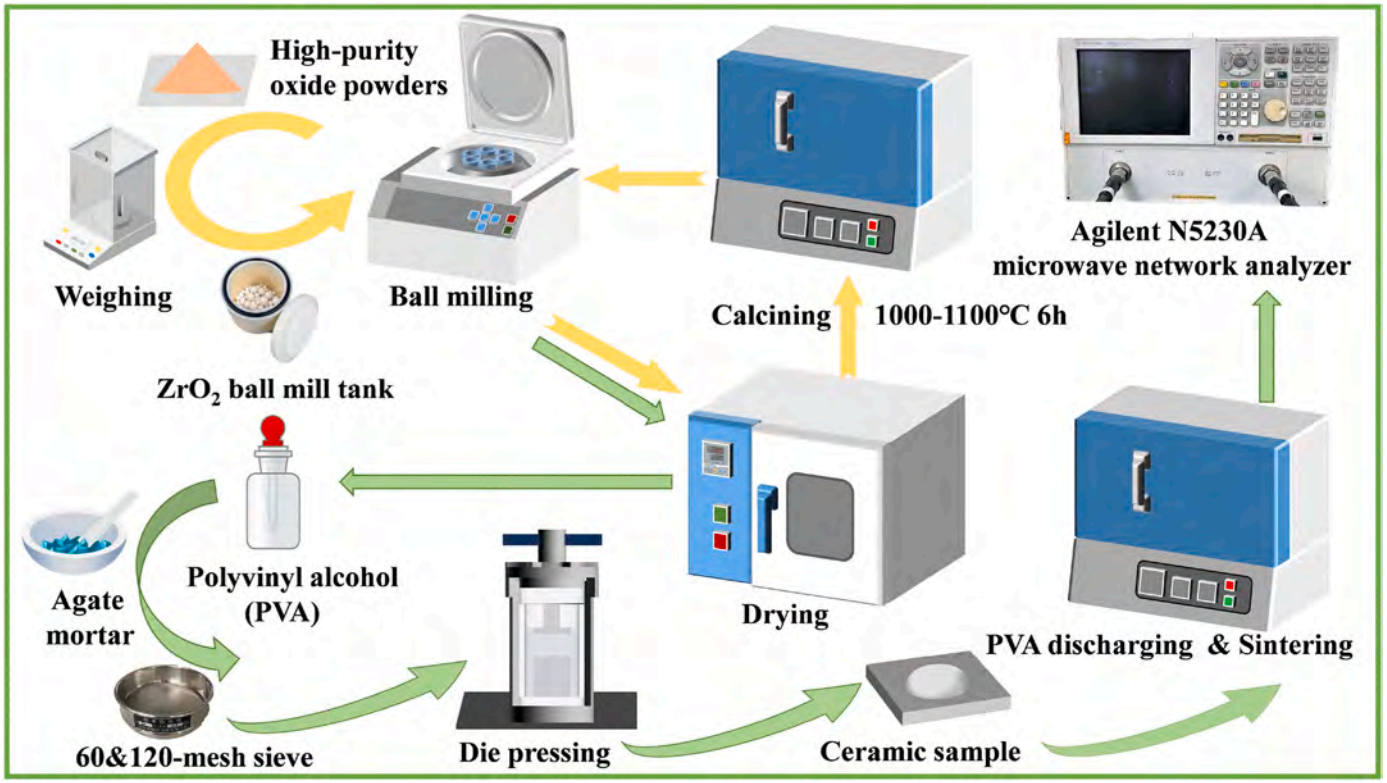

Fig. 2. The experimental procedure for the synthesis of $CaEuGaO_4$ and $CaEuAlO_4$ ceramics.

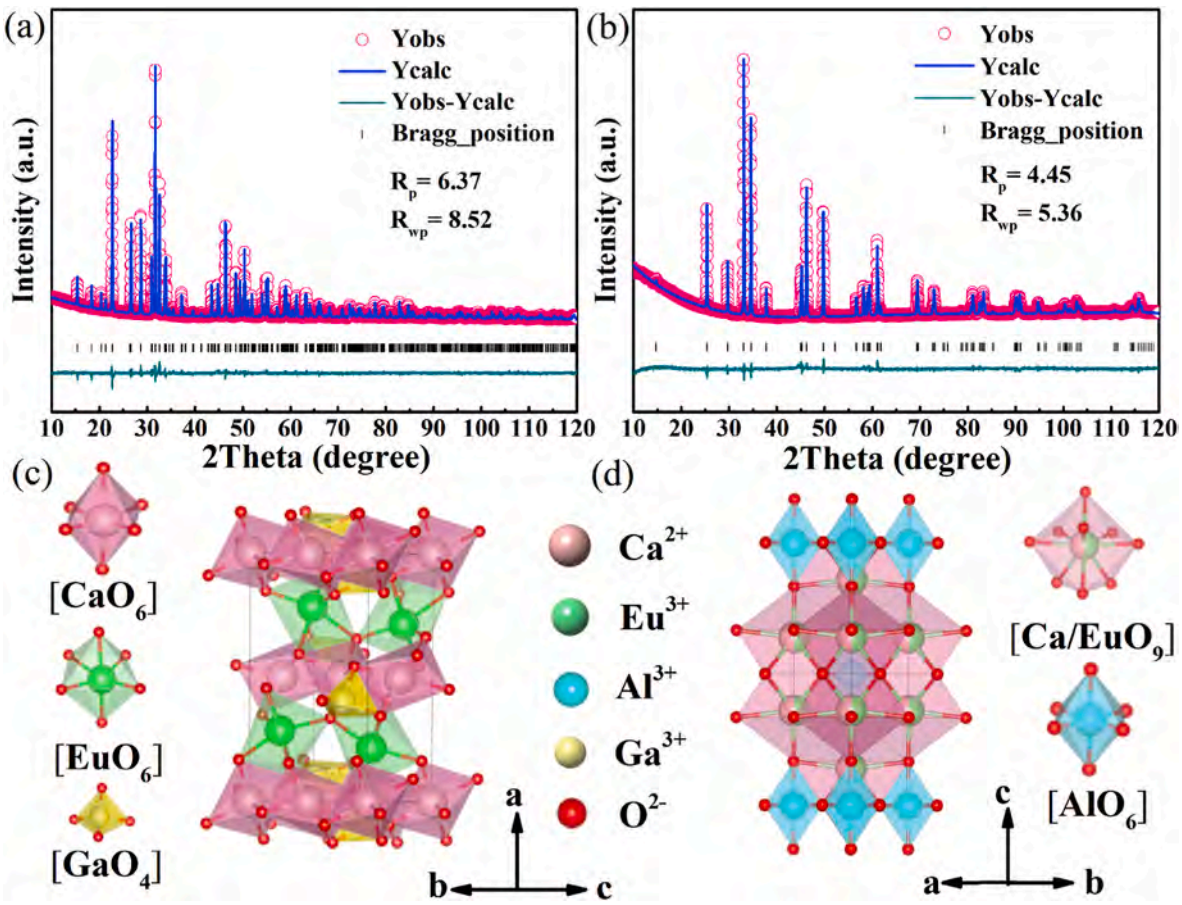

Fig. 4. Rietveld refinement plots of (a) $CaEuGaO_4$ and (b) $CaEuAlO_4$ ceramics. Schematics of the crystal structures of (c) olivine $CaEuGaO_4$ and (d) tetragonal $CaEuAlO_4$.

Table 1
Crystallographic data of $CaEuGaO_4$ and $CaEuAlO_4$ derived from the Rietveld refinement.

Ceramics	Atoms	Wyckoff positions	*x*	*y*	*z*	Occupancy
$CaEuGaO_4$	Ca	4*a*	0.5000	0.5000	0.5000	1
	Eu	4*c*	0.2209	0.2500	0.5066	1
	Ga	4*c*	0.4041	0.2500	0.0597	1
	O1	4*c*	0.5503	0.2500	0.2191	1
	O2	4*c*	0.4084	0.2500	0.7351	1
	O3	8*d*	0.3436	0.4567	0.2307	1
Crystal System			Orthorhombic *pnma* (No. 62)			
Space Group			$a = 11.498$ Å, $b = 6.679$ Å, $c = 5.314(7)$ Å			
Lattice Parameter			$V = 408.089(7)$ Å^3, $Z = 4$			
Volume, *Z*						
$CaEuAlO_4$	Ca	4*e*	0.0000	0.0000	0.3584	0.5
	Eu	4*e*	0.0000	0.0000	0.3584	0.5
	Al	2*a*	0.0000	0.0000	0.0000	1
	O1	4*c*	0.0000	0.5000	0.0000	1
	O2	4*e*	0.0000	0.0000	0.1677	1
Crystal System			Tetragonal			
Space Group			*I4/mmm* (No. 139) $a = b = 3.666$ Å, $c =$ 12.024(2) Å			
Lattice Parameter						
Volume, *Z*			$V = 161.606(2)$ Å^3, $Z = 2$			

$$\tau_f = \frac{f_{85} - f_{25}}{f_{25} \times (85°C - 25°C)} \quad (1)$$

$$\tau_\varepsilon = \frac{\varepsilon_{r85} - \varepsilon_{r25}}{\varepsilon_{r25} \times (85°C - 25°C)} \quad (2)$$

3. Results and discussion

$CaEuGaO_4$ powder diffraction patterns are consistent with the olivine structure (PDF # 00-27-1050), as shown in Fig. 3, while $CaEuAlO_4$ crystallized into a tetragonal phase with *I4/mmm* space group (PDF # 00-024-0190). As the Ln^{3+} radius decreases, the diffraction peaks shift to higher angles. To elucidate the crystal structures of $CaEuGaO_4$ and $CaEuAlO_4$, a Rietveld refinement was performed on the powder diffraction patterns (Fig. 4a and b). Results show a good fit to an orthorhombic $CaEuGaO_4$ with lattice constants $a = 11.498$ Å, $b = 6.679$ Å, and $c = 5.314(7)$ Å and a tetragonal $CaEuAlO_4$ with lattice constants $a = b = 3.666$ Å and $c = 12.024(2)$ Å. Table 1 summarizes the refined parameters, Wyckoff sites, and occupation of atoms, respectively. The crystal structure of the olivine $CaEuGaO_4$ is shown in Fig. 4c. Ca^{2+} and Eu^{3+} cations filled the octahedral sites, whereas Ga^{3+} cations occupied the tetrahedral sites along the *b*-axis, and O^{2-} cations formed a hexagonal tight packing along the *b*-axis. Tetragonal $CaEuAlO_4$ can be described as the perovskite layer $(Ca/Eu)AlO_3$ and the rock salt layer Ca/EuO stacked at a ratio of 1:1, where Eu^{3+} and Ca^{2+} co-occupy the dodecahedron of 9 coordination while Al^{3+} occupies the octahedron of 6 coordination (Fig. 4d). The $[AlO_6]$ octahedrons of the same layer were connected with each other by co-apex, and the Ca/La cations with a larger ionic radius were located in the voids formed by the $[AlO_6]$ octahedron [11,27].

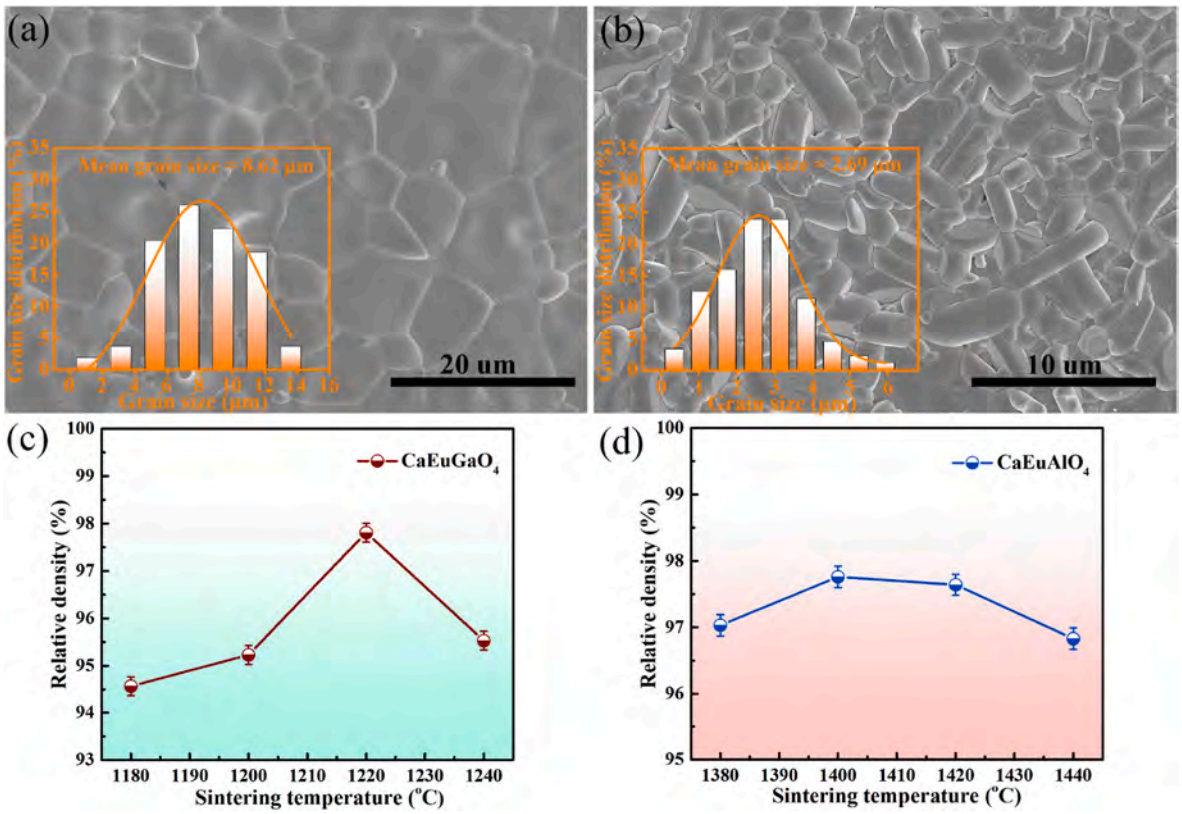

Fig. 5. SEM images of the thermal etched surfaces of (a) $CaEuGaO_4$ sintered at 1220 °C and (b) $CaEuAlO_4$ sintered at 1400 °C. Sintering temperature dependence of relative density of (c) $CaEuGaO_4$ and (d) $CaEuAlO_4$.

Fig. 5 shows the SEM images of $CaEuGaO_4$ and $CaEuAlO_4$ ceramics. The microstructures of both ceramics sintered at optimal temperatures are homogeneous and dense. The grain boundaries of $CaEuGaO_4$ ceramics are clear, and the grains are typical orthorhombic irregular granular, while the grains of $CaEuAlO_4$ ceramics are typical tetragonal rods. Increasing the sintering temperature accelerated the densification of ceramics, with saturated values of 97.81 % for $CaEuGaO_4$ sintered at 1220 °C and 97.76 % for $CaEuAlO_4$ sintered at 1400 °C (Fig. 5c and d).

The ε_r, $Q \times f$, and τ_f of $CaEuGaO_4$ and $CaEuAlO_4$ ceramics were originally raised to the maximum values and subsequently reduced as the sintering temperature increased (Fig. 6), which is the influence of extrinsic factors (porosity) on the microwave dielectric properties. At the optimum sintering temperature, the sample has the lowest porosity and the effect of extrinsic influences may be neglected [28–30]. The measured permittivities ε_r of $CaEuGaO_4$ and $CaEuAlO_4$ are 9.7 (1220 °C) and 19.1 (1400 °C), respectively. According to the Bosma-Havinga equation [31], the corrected permittivities $\varepsilon_{r(\mathrm{Corr})}$ (10.1 and 19.7) of $CaEuGaO_4$ and $CaEuAlO_4$ after eliminating pores can be obtained.

$$\varepsilon_{r(\mathrm{Corr})} = \varepsilon_r(1 + 1.5P) \tag{3}$$

It is obvious that the ε_r of orthorhombic olivine $CaEuGaO_4$ is much lower than that of tetragonal K_2NiF_4-type $CaEuAlO_4$. The variation of ε_r could be explained by Shannon's additive rule and the Clausius-Mossotti connection:

$$\alpha_m\ (ABCO_4) = \alpha(A) + \alpha(B) + \alpha(C) + 4\alpha(O) \tag{4}$$

$$\varepsilon_{r(\mathrm{C-M})} = \frac{3V_m + 8\pi\alpha_m}{3V_m - 4\pi\alpha_m} \tag{5}$$

where V_m is the molar unit-cell volume and α_m is the total of the ionic polarizability [32]. The difference between the corrected $\varepsilon_{r(\mathrm{Corr})}$ (10.1 and 19.7) and the calculated $\varepsilon_{r(\mathrm{C\text{-}M})}$ (8.4 and 18.9) of $CaEuGaO_4$ and $CaEuAlO_4$ may occur because of the "rattling" cations.

As listed in Table 2, the deviations between the $\varepsilon_{r(\mathrm{Corr})}$ and $\varepsilon_{r(\mathrm{C\text{-}M})}$ are 20.24 % for $CaEuGaO_4$ and 4.23 % for $CaEuAlO_4$, respectively. The oxide additivity rule (Eq. (4)) yields dielectric polarizabilities (α_m) that differ by 5.69 % and 0.61 % from those observed (α_{obs}). Positive deviations greater than 5 % have previously been discovered to suggest peculiar physical characteristics, including ionic or electronic conductivity, piezoelectric resonance, or peculiar structural features [33]. The evaluation of cation bond valences is one method that is effective for interpreting deviations in additivity in cubic garnets and spinels. The bond valence v_{ij} (associated with cation-anion interaction) of the bond formed between two ions i and j with opposite charges is defined as follows [34]:

$$v_{ij} = \exp\left(\frac{R_{ij} - d_{ij}}{b}\right) \tag{6}$$

where R_{ij} is the bond valence parameter, b is the empirical constant equal to 0.37, and d_{ij} is the cation-anion bond length [35]. Following is a notation for the i^{th} ion's bond valence sum (V_i):

$$V_i = \sum_j v_{ij} \tag{7}$$

Table 3 compares the bond valence of each cation in $CaEuGaO_4$ and $CaEuAlO_4$. Ca^{2+} is in a "compressed" state, as the bond valence of Ca^{2+} in $CaEuGaO_4$ is 2.336 *v.u.*, which is greater than the ideal value of 2.000 *v.u.* The Ga^{3+} (3.318 *v.u.*) is obviously in a "compressed" state as well. The bond valence of Eu^{3+} (2.330 *v.u.*) is lower than the ideal value (3.000 *v.u.*), indicating the "rattling" state of Eu^{3+}. A similar situation in $CaEuAlO_4$ ceramics is that Ca^{2+} is in a "compressed" state with bond valence (2.058 *v.u.*) marginally exceeding the ideal value (2.000 *v.u.*). The bond valence of Eu^{3+} and Al^{3+} in a dodecahedron (2.748 and 2.934 *v.u.*) are both lower than 3.000 *v.u.* (ideal value), both in a slightly "rattling" state.

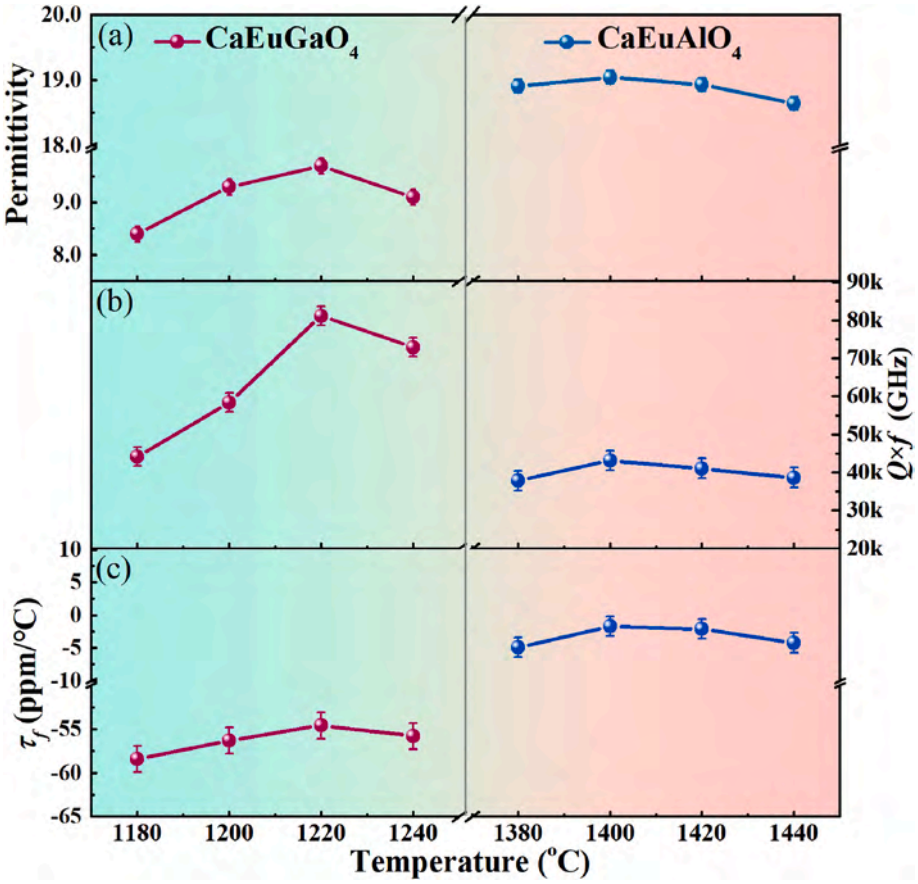

Fig. 6. Microwave dielectric properties of $CaEuGaO_4$ and $CaEuAlO_4$ ceramics as a function of sintering temperature.

Table 2
Relative permittivities and molar polarizabilities of $CaEuGaO_4$ and $CaEuAlO_4$.

Ceramics	α_m (Å^3)	V_m (Å^3)	α_m/V_m	$\varepsilon_{r(C\text{-}M)}$	ε_r	$\varepsilon_{r(Corr)}$	α_{obs}	$\Delta\varepsilon_r$	$\Delta\alpha$
$CaEuGaO_4$	17.23	102.02	0.163	8.4	9.7	10.1	18.21	20.24 %	5.69 %
$CaEuAlO_4$	16.52	80.81	0.204	18.9	19.1	19.7	16.62	4.23 %	0.61 %

Table 3
The bond valences of $CaEuGaO_4$ and $CaEuAlO_4$.

Ceramics	Atom	Bond	d_{ij} (Å)	V_i (*v. u.*)	Ideal V_i (*v. u.*)	V_i deviation
$CaEuGaO_4$	Ca	Ca–O1*2	2.526	2.336	2.000	16.80 %
		Ca–O2*2	2.313			
		Ca–O3*2	2.185			
	Eu	Eu-O1	2.452	2.330	3.000	−22.33 %
		Eu-O2	2.571			
		Eu-O3*2	2.443			
		Eu-O3'*2	2.346			
	Ga	Ga-O1	1.894	3.318	3.000	10.60 %
		Ga-O2	1.890			
		Ga-O3*2	1.725			
$CaEuAlO_4$	Ca	Ca–O1*4	2.502	2.058	2.000	2.90 %
		Ca–O2*4	2.611			
		Ca–O2′	2.293			
	Eu	Eu-O1*4	2.502	2.748	3.000	−8.40 %
		Eu-O2*4	2.611			
		Eu-O2′	2.293			
	Al	Al–O1*4	1.833	2.934	3.000	−2.20 %
		Al–O2*2	2.016			

Table 4
The effective ionic radii, unit cell volume, and packing fraction in $CaEuGaO_4$ and $CaEuAlO_4$.

Ceramics	r_{Ca}^{2+} (Å) (*CN* = 6)	r_{Eu}^{3+} (Å) (*CN* = 6)	r_{Ga}^{3+} (Å) (*CN* = 4)	r_{O}^{2-} (Å) (*CN* = 4)	V (Å^3)	Z	Packing fraction
$CaEuGaO_4$	1.000	0.947	0.470	1.380	408.089	4	51.18 %
	r_{Ca}^{2+} (Å) (*CN* = 9)	r_{Eu}^{3+} (Å) (*CN* = 9)	r_{Al}^{3+} (Å) (*CN* = 6)	r_{O}^{2-} (Å) (*CN* = 6)			
$CaEuAlO_4$	1.180	1.120	0.535	1.400	166.606	2	73.61 %

CaEuGaO4 sintered at 1220 °C and CaEuAlO4 sintered at 1400 °C yield maximal Q × f values of 82,049 and 43,132 GHz, respectively (Fig. 6b). The $Q \times f$ is highly dependent on structural characteristics such as packing fraction, bond strength (S), and covalence (f_c) [36]. From the ionic radius and the primitive unit cell volume, it is possible to calculate the packing fraction:

$$\text{Packing fraction} = \frac{V_A + V_B + V_C + V_O}{V} \times Z \quad (8)$$

Table 5
Calculation parameters and bond covalency of $CaEuGaO_4$ and $CaEuAlO_4$.

Ceramics	Atom	R_1	N	S	f_c (%)
$CaEuGaO_4$	Ca	1.799	4.483	0.307	24.99
	Eu	2.090	6.500	0.371	27.88
	Ga	1.746	6.050	0.808	53.94
$CaEuAlO_4$	Ca	1.799	4.483	0.216	20.45
	Eu	2.090	6.500	0.287	24.06
	Al	1.622	4.290	0.428	31.37

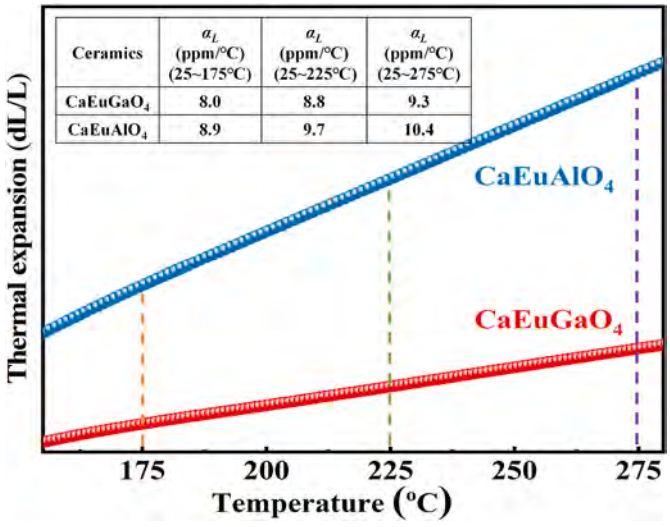

Fig. 7. Thermal expansion data of $CaEuGaO_4$ and $CaEuAlO_4$ ceramics.

where V_A, V_B, V_C, and V_O are the volume of ions at each site, and $Z = 4$ and 2 for the olivine-type and K_2NiF_4-type ceramic, and the specific parameters are listed in Table 4. The packing fractions of $CaEuGaO_4$ and $CaEuAlO_4$ are 51.18 % and 73.61 %, respectively, which is opposite to their $Q \times f$ variation. Kim et al. [37] found that $Q \times f$ is related to the packing fraction in scheelite-structured ABO_4 (A = Ca, Pb, Ba; B═Mo, W) ceramics. The opposite phenomenon in $CaEuGaO_4$ and $CaEuAlO_4$ ceramics demonstrates that other factors also affect their $Q \times f$ values.

A decrease in the intrinsic losses of ceramics may result from the strong bonding between cations and oxygen ions, i.e., high covalency [38]. The following empirical equations may be used to characterize the connection between the covalence (f_c) and bond strength (S) for $M - O$ bonds [36]:

$$S = (R/R_1)^{-N} \tag{9}$$

$$f_c = aS^M \tag{10}$$

where R is the average cation-oxygen ion bond length, R_1 and N rely on the cation site, and a and M depend on electrons. As shown in Table 5, the f_c of Ca–O in $CaEuCO_4$ (C═Ga, Al) turns weaker from 24.99 % to 20.45 %, Eu–O from 27.88 % to 24.06 %, and C–O from 53.94 % to 31.37 %, which correlates with higher bond strength in $CaEuCO_4$. Therefore, the higher bond strength may be the main reason for the higher $Q \times f$ in $CaEuGaO_4$ ceramic.

Both $CaEuGaO_4$ and $CaEuAlO_4$ had low sensitivity to changes in sintering temperature (Fig. 6c), with τ_f values of −54.6 ppm/°C and −1.6 ppm/°C, respectively. Commonly, τ_f is associated with the temperature coefficient of permittivity (τ_ε) and the linear coefficient of thermal expansion (α_L), as follows [39,40]:

$$\tau_f = -\left(\frac{\tau_\varepsilon}{2} + \alpha_L\right) \tag{11}$$

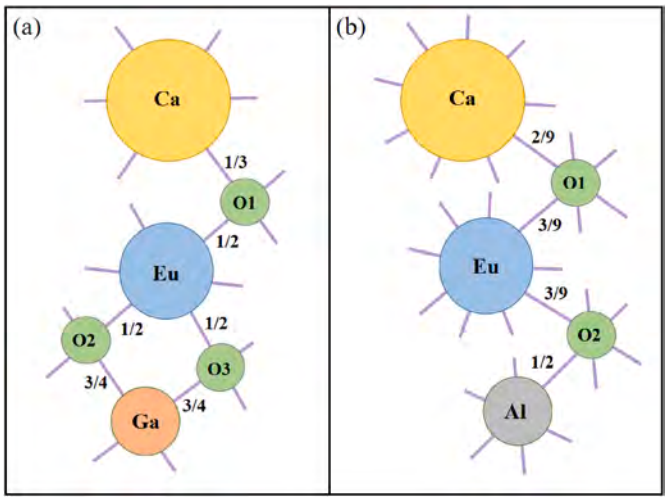

Fig. 8. Chemical bond charge balance diagram of (a) $CaEuGaO_4$ (b) $CaEuAlO_4$ ceramics.

$$\tau_\varepsilon = \frac{1}{\varepsilon_r}\left(\frac{\partial \varepsilon_r}{\partial T}\right) = \frac{(\varepsilon_r - 1)(\varepsilon_r + 2)}{3\varepsilon_r}\left(\frac{1}{\alpha_m}\frac{d\alpha_m[T, V(T)]}{dT} - 3\alpha_L\right) = \frac{(\varepsilon_r - 1)(\varepsilon_r + 2)}{3\varepsilon_r}(\tau_{\alpha m} - 3\alpha_L) \tag{12}$$

As depicted in Fig. 7, the α_L of $CaEuCO_4$ (C═Ga, Al) increases as the temperature rises, with measured α_L values of +9.3 and + 10.4 ppm/°C, respectively. The calculated τ_ε values are +90.6 ppm/°C for $CaEuGaO_4$ and -17.6 ppm/°C for $CaEuAlO_4$ between 25 °C and 85 °C. Apparently, the absolute value of τ_ε is larger than α_L and has a significant impact on τ_f. $CaEuCO_4$ (C═Ga, Al) ceramics have positive and deterministic ε_r and α_L, therefore the value of $\tau_{\alpha m}$-$3\alpha_L$ mostly affects the signs and magnitudes of their τ_ε and τ_f. The $\tau_{\alpha m}$ is 53.80 ppm/°C for $CaEuGaO_4$ and 28.53 ppm/°C for $CaEuAlO_4$, respectively. A higher τ_ε in $CaEuGaO_4$ ceramic results in lower τ_f and higher $\tau_{\alpha m}$ compared to $CaEuAlO_4$.

The P–V-L chemical bond theory was used to further investigate the connection between the chemical bond characteristics of $CaEuGaO_4$ and $CaEuAlO_4$ ceramics and the modifications to their microwave dielectric properties [41]. The chemical bond formula of $CaEuGaO_4$ and $CaEuAlO_4$ ceramics can be decomposed into the following binary bond subformula [42,43], and the charge balance of chemical bonds in the $CaEuGaO_4$ and $CaEuAlO_4$ ceramics is shown in Fig. 8. In $CaEuGaO_4$ and $CaEuAlO_4$ ceramics, the effective valence electron numbers of Ca, Eu, and Ga are $Z_{Ca} = 2$, $Z_{Eu} = 3$, $Z_{Ga} = 3$, and $Z_{Al} = 3$. And the effective valence electron numbers of the O^{2-} anion should be followed by the subformula.

$$\begin{aligned} CaEuGaO_4 ═ & Ca_{1/3}O(1)_{1/2} + Ca_{1/3}O(2)_{1/2} + Ca_{1/3}O(3)_{1/2} \\ & + Eu_{1/6}O(1)_{1/4} + Eu_{1/6}O(2)_{1/4} + Eu_{1/3}O(3)_{1/2} + Eu_{1/3}O(3)'_{1/2} \\ & + Ga_{1/4}O(1)_{1/4} + Ga_{1/4}O(2)_{1/4} + Ga_{1/2}O(3)_{1/2} \end{aligned} \tag{13}$$

$$\begin{aligned} CaEuAlO_4 ═ & Ca_{4/9}O(1)_{2/3} + Ca_{4/9}O(2)_{2/3} + Ca_{1/9}O(2')_{1/6} \\ & + Eu_{4/9}O(1)_{2/3} + Eu_{4/9}O(2)_{2/3} + Eu_{1/9}O(2')_{1/6} \\ & + Al_{2/3}O(1)_{2/3} + Al_{1/3}O(2)_{1/3} \end{aligned} \tag{14}$$

The bond ionicity (f_i) and susceptibility (χ) are relative to ionic polarization which in microwave frequency is closely tied to the dielectric constant, and can be calculated to determine the contribution of different bonds in ε_r [44]:

$$f_i = \frac{(C^\mu)^2}{\left(E_g^\mu\right)^2} = \frac{(C^\mu)^2}{(E_h^\mu)^2 + (C^\mu)^2} \tag{15}$$

Table 6
Calculated ionicity (f_i) and lattice energy (U) values of each chemical bond in $CaEuGaO_4$ and $CaEuAlO_4$ ceramics through the P–V-L theory.

Ceramics	Bond type	f_i	U (kJ/mol)	ε^{μ}	χ^{μ}	χ	$\chi/\sum\chi$
$CaEuGaO_4$	Ca–O1 × 2	0.7798	973.05	3.85	0.2272	0.0284	10.13 %
	Ca–O2 × 2	0.7722	1044.24	3.48	0.1971	0.0246	8.78 %
	Ca–O3 × 2	0.7664	1092.27	3.27	0.1804	0.0226	8.04 %
	Eu-O1 × 1	0.8474	1083.45	4.16	0.2517	0.0157	5.61 %
	Eu-O2 × 1	0.8490	1043.08	4.44	0.2738	0.0171	6.10 %
	Eu-O3 × 2	0.8472	2173.25	4.14	0.2501	0.0313	11.15 %
	Eu-O3' × 2	0.8455	2244.09	3.93	0.2333	0.0292	10.40 %
	Ga-O1 × 1	0.6313	2229.18	7.05	0.4813	0.0301	10.73 %
	Ga-O2 × 1	0.6311	2232.57	7.03	0.4796	0.0300	10.69 %
	Ga-O3 × 2	0.6200	4761.97	6.18	0.4122	0.0515	18.37 %
	$\chi_{(Ca-O)}$				0.6047	0.0756	26.95 %
	$\chi_{(Eu-O)}$				1.0089	0.0933	33.26 %
	$\chi_{(Ga-O)}$				1.3731	0.1116	39.79 %
	Total		18877.14		2.9867	0.2804	
$CaEuAlO_4$	Ca–O1 × 4	0.6645	1330.20	7.57	0.5230	0.0872	12.95 %
	Ca–O2 × 4	0.6669	1285.63	8.10	0.5653	0.0942	14.00 %
	Ca–O2' × 1	0.6579	356.34	6.63	0.4483	0.0187	2.78 %
	Eu-O1 × 4	0.7539	2843.01	9.24	0.6557	0.1093	16.24 %
	Eu-O2 × 4	0.7544	2747.82	9.95	0.7124	0.1187	17.65 %
	Eu-O2' × 1	0.7514	761.27	7.99	0.5568	0.0232	3.45 %
	Al–O1 × 4	0.5354	5982.22	11.47	0.8335	0.1389	20.64 %
	Al–O2 × 2	0.5418	2790.43	13.47	0.9923	0.0827	12.29 %
	$\chi_{(Ca-O)}$				1.5367	0.2001	29.73 %
	$\chi_{(Eu-O)}$				1.9250	0.2512	37.34 %
	$\chi_{(Al-O)}$				1.8258	0.2216	32.93 %
	Total		18096.90		5.2875	0.6729	

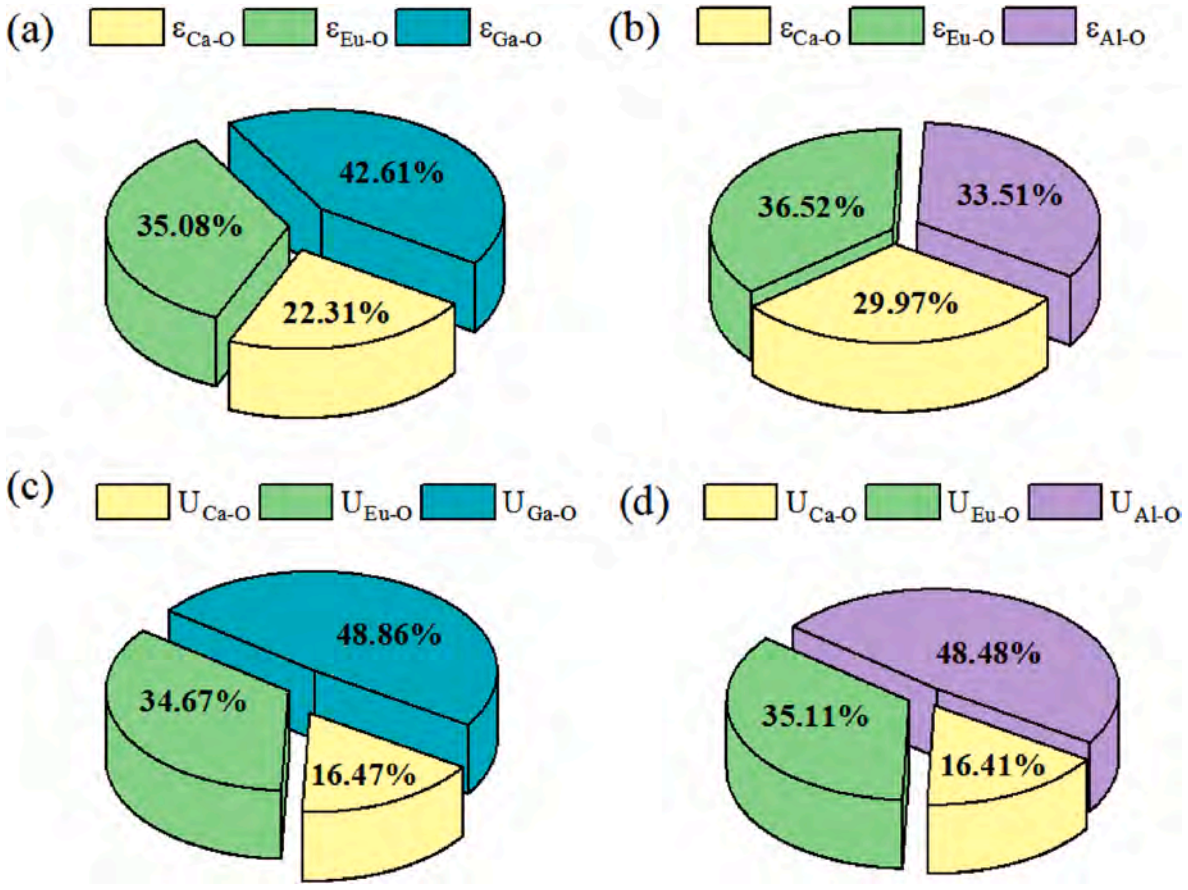

Fig. 9. Contribution of each chemical bond to the ε and to the U of (a) (c) $CaEuGaO_4$, (b) (d) $CaEuAlO_4$ ceramics.

$$\chi = \sum_{\mu} F^{\mu} \cdot \chi^{\mu} = \sum_{\mu} N_b^{\mu} \cdot \chi_b^{\mu} \tag{16}$$

$$\chi^{\mu} = \frac{\left(h\Omega_p^{\mu}\right)^2}{4\pi\left(E_g^{\mu}\right)^2} \tag{17}$$

$$\varepsilon^{\mu} = 1 + 4\pi\chi^{\mu} \tag{18}$$

where C^{μ}, E_h^{μ}, and E_g^{μ} refer to the heteropolar, homopolar, and average energy gap, h is Planck's constant, Ω_p^{μ} is the plasma frequency, F^{μ} is the fraction of bonds of type μ composing the actual complex crystal, and N_b^{μ} is the number of bonds per cubic centimeter, which can be obtained from the crystal structural data. The lattice energy (U) considering the contributions of the ionic (U_{bi}^{μ}) and covalent (U_{bc}^{μ}) parts of the chemical bond is calculated as follows:

$$U = \sum_{\mu}(U_{bi}^{\mu} + U_{bc}^{\mu}) \tag{19}$$

In both $CaEuGaO_4$ and $CaEuAlO_4$ ceramics, the Eu–O bond in the B site has the strongest ionicity (f_i), with an average ionicity (Af_i) of 84.73 % (orthorhombic olivine) and 75.32 % (perovskite-like structure), respectively (Table 6). The chemical bond contributions to the permittivity of $CaEuGaO_4$ are presented in Fig. 9a in the following order: Ga–O > Eu–O > Ca–O. The contribution order of chemical bonds to the ε_r of $CaEuAlO_4$ is Eu–O > Al–O > Ca–O (Fig. 9b). In addition, the calculated results of χ^{μ} and χ can specifically reflect the contribution of each type of chemical bond to the dielectric polarization ability, among which the Ga–O bond contributes about 39.79 %. In comparison, Eu–O and Ca–O bonds contribute about 33.26 % and 26.95 %, indicating that the Ga–O bond plays a dominant role in the relative permittivity of $CaEuGaO_4$. And in $CaEuAlO_4$ ceramics, Eu–O bond contributes the most about 37.34 % compared with Ca–O and Al–O bonds about 29.73 % and 32.93 %. The binding strength of anions and cations is reflected in the lattice energy (U). If a crystal has high binding energy, it will be stable and have less intrinsic loss [45,46]. Table 6 displays the computed U values for the chemical bonds. According to the ranking of the U values of the chemical bonds (Fig. 9c and d), the Ga(Al)–O bonds contribute the most to the lattice energy, followed by the Eu–O bonds and the Ca–O bonds.

4. Conclusions

$CaEuGaO_4$ with orthorhombic olivine structure (*pnma*) and $CaEuAlO_4$ with tetragonal perovskite-like structure (*I4/mmm*, K_2NiF_4-type) were prepared by the solid-state reaction, and a high relative density (~97 %) was obtained. The difference in their structures is mainly caused by the properties of the Ga (III) atom, which can exhibit octahedral and tetrahedral coordination through the oxygen atom. However, the space group *I4mm* allows Ga atoms to deviate from the center of the octahedron, which leads to the formation of [GaO_4] tetrahedra, i.e., the transition from *I4mm* to *pnma*. $CaEuGaO_4$ ceramics have a low ε_r (9.7), a higher $Q\times f$ (82,049 GHz), and a large negative τ_f value (−54.6 ppm/°C). $CaEuAlO_4$ ceramics have a higher ε_r (18.9), a lower $Q\times f$ (43,132 GHz), and a near-zero negative τ_f (−1.6 ppm/°C). The ε_r of $CaEuCO_4$ (C═Ga, Al) is closely related to the change of ionic polarizability per unit volume (α_m/V_m). The difference between the corrected $\varepsilon_{r(Corr)}$ (10.1 and 19.7) and the calculated $\varepsilon_{r(C\text{-}M)}$ (8.4 and 18.9) of $CaEuGaO_4$ and $CaEuAlO_4$ may occur because of the "rattling" cations. Due to the strong covalency between cations and oxygen ions in the chemical bonds of $CaEuGaO_4$ ceramics, its $Q\times f$ value is higher than that of $CaEuAlO_4$. A higher τ_ε in $CaEuGaO_4$ ceramic results in lower τ_f and higher $\tau_{\alpha m}$ compared to $CaEuAlO_4$, i.e., $\tau_{\alpha m}$-$3\alpha_L$ values affect the magnitude and sign of τ_ε and τ_f.

Declaration of competing interest

The authors declare that they have no known competing financial interests or personal relationships that could have appeared to influence the work reported in this paper.

Acknowledgments

This work was funded by the Natural Science Foundation of Guangxi Zhuang Autonomous Region (Nos. 2023GXNSFBA026076, 2022GXNSFBA035602), the National Natural Science Foundation of China (Nos. 21965009 and 22105048), the Guangxi Key Laboratory of Optical and Electronic Materials and Devices (No. 22 KF-10), the Guilin University of Technology Research Startup Project (No. GUTQDJJ2021073), and Guangxi BaGui Scholars Special Funding.

References

[1] H. Ronde, D.M. Krol, G. Blasse, The luminescence of Eu^{3+} and Bi^{3+} in the two modifications of $CaLaGaO_4$, J. Am. Ceram. Soc. 124 (1977) 1276–1280.
[2] W.S. Fang, J.Q. Chen, Y. Yang, L.Y. Ao, Y. Tang, J. Li, L. Fang, Anomalous microwave dielectric behaviour induced by the orthorhombic-tetragonal phase transition in $CaLaGaO_4$ ceramics, J. Eur. Ceram. Soc. 42 (2022) 1474–1479.
[3] R. Clark, J.X. Zhu, S.T. Zheng, X.H. Bu, S. Derakhshan, $CaYGaO_4$: a fully ordered novel olivine type gallate, J. Alloys Compd. 616 (2014) 340–344.
[4] W.S. Fang, Y. Yang, H.C. Xiang, Y. Tang, J. Li, L. Fang, Correlation between structure and microwave dielectric properties of ordered olivine $CaLnGaO_4$ (Ln = Pr, Yb) ceramics, Ceram. Int. 49 (2023) 32008–32014.
[5] R. Brown, V. Pendrick, D. Kalokitis, B.H.T. Chai, Low-loss substrate for microwave application of high-temperature superconductor films, Appl. Phys. Lett. 57 (1990) 1351–1353.
[6] R. Sobolewski, P. Gierlowski, W. Kula, S. Zarembihki, S.J. Lewandowski, M. Berkowski, A. Pajqczkowska, High-Tc thin films on low microwave loss alkaline rare-earth-aluminate crystals, IEEE Trans. Magn. 27 (1991) 876–879.
[7] K. Nakamura, I. Aoyama, R. Katuno, LaSrGaO4 substrate for epitaxial high-Tc superconducting thin films, Phase Transitions 42 (1993) 99–102.
[8] Z.F. Li, G.B. Li, F.H. Liao, J.H. Lin, On the synthesis and structure of $LaCaGaO_4$, J. Solid State Chem. 172 (2003) 59–65.
[9] X.M. Chen, X.Q. Liu, Microwave dielectric characteristics of $SrLaGaO_4$ and $SrNdGaO_4$ ceramics, J. Eur. Ceram. Soc. 26 (2006) 1969–1971.
[10] Y. Xiao, X.M. Chen, X.Q. Liu, Microstructures and microwave dielectric characteristics of $CaRAlO_4$ (R = Nd, Sm, Y) ceramics with tetragonal K_2NiF_4 structure, J. Am. Ceram. Soc. 87 (2004) 2143–2146.
[11] X.C. Fan, X.M. Chen, X.Q. Liu, Structural dependence of microwave dielectric properties of $SrRAlO_4$ (R = Sm, Nd, La) ceramics: crystal structure refinement and infrared reflectivity study, Chem. Mater. 20 (2008) 4092–4098.
[12] P. Byszewski, J. Domagała, J. Fink-Finowicki, A. Pajaczkowska, Thermal properties of $CaNdAlO_4$ and $SrLaAlO_4$ single crystals, Mater. Res. Bull. 27 (1992) 483–490.
[13] X.Q. Liu, X.M. Chen, Y. Xiao, Preparation and characterization of $LaSrAlO_4$ microwave dielectric ceramics, Mater. Sci. Eng., B 103 (2003) 276–280.
[14] X.M. Chen, Y. Xiao, X.Q. Liu, X. Hu, $SrLnAlO_4$ (Ln = Nd and Sm) microwave dielectric ceramics, J. Electroceram. 10 (2003) 111–115.
[15] L. Yi, L. Li, X.M. Chen, Structures and microwave dielectric characteristics of compounds in vicinity of $CaNdAlO_4$ in CaO-Nd_2O_3-Al_2O_3 ternary system, Adv. Appl. Ceram. 112 (2013) 46–52.
[16] R.D. Shannon, R.A. Oswald, J.B. Parise, B.H.T. Chai, P. Byszewski, A. Pajaczkowska, R. Sobolewski, Dielectric-constants and crystal-structures of $CaYAlO_4$, $CaNdAlO_4$, and $SrLaAlO_4$, and deviations from the oxide additivity rule, J. Solid State Chem. 98 (1992) 90–98.
[17] E.L. Colla, I.M. Reaney, N. Setter, Effect of structural changes in complex perovskites on the temperature coefficient of the relative permittivity, J. Appl. Phys. 74 (1993) 3414–3425.
[18] I.M. Reaney, E. Colla, N. Setter, Dielectric and structural characteristics of Ba-and Sr-based complex perovskites as a function of tolerance factor, Jpn. J. Appl. Phys. 33 (1994) 3984.
[19] J.C. Kim, M.H. Kim, S. Nahm, J.H. Paik, J.H. Kim, H.J. Lee, Synthesis and microwave dielectric properties of $Re_3Ga_5O_{12}$ (Re: Nd, Sm, Eu, Dy, Yb, and Y) ceramics, J. Am. Ceram. Soc. 90 (2007) 641–644.
[20] A. Sunny, V. Viswanath, K.P. Surendran, M.T. Sebastian, The effect of Ga^{3+} addition on the sinterability and microwave dielectric properties of $RE_3Al_5O_{12}$ (Tb^{3+}, Y^{3+}, Er^{3+} and Yb^{3+}) garnet ceramics, Ceram. Int. 40 (2014) 4311–4317.
[21] J.J. Xue, S.P. Wu, J.H. Li, Synthesis, microstructure, and microwave dielectric properties of spinel $ZnGa_2O_4$ ceramics, J. Am. Ceram. Soc. 96 (2013) 2481–2485.
[22] S.P. Wu, J.J. Xue, R. Wang, J.H. Li, Synthesis, characterization and microwave dielectric properties of spinel $MgGa_2O_4$ ceramic materials, J. Alloys Compd. 585 (2014) 542–548.
[23] A. Kan, T. Moriyama, S. Takahashi, H. Ogawa, Cation distributions and microwave dielectric properties of spinel-structured $MgGa_2O_4$ ceramics, Jpn. J. Appl. Phys. 52 (2013), 09KH01.
[24] K.P. Surendran, N. Santha, P. Mohanan, M.T. Sebastian, Temperature stable low loss ceramic dielectrics in (1-x)$ZnAl_2O_4$-$x$$TiO_2$ system for microwave substrate applications, Eur. Phys. J. B 41 (2004) 301–306.
[25] K.P. Surendran, P.V. Bijumon, P. Mohanan, M.T. Sebastian, (1-x)$MgAl_2O_4$-$x$$TiO_2$ dielectrics for microwave and millimeter wave applications, Appl. Phys. A 81 (2005) 823–826.
[26] W.E. Courtney, Analysis and evaluation of a method of measuring the complex permittivity and permeability microwave insulators, IEEE. T. Microw. Theory 18 (1970) 476–485.

[27] A. Pajaczkowska, A. Gloubokov, Synthesis, growth and characterization of tetragonal $ABCO_4$ crystals, Prog. Cryst. Growth Char. 36 (1998) 123–162.
[28] N.M. Alford, J. Breeze, X. Wang, S.J. Penn, S. Dalla, S.J. Webb, N. Ljepojevic, X. Aupi, Dielectric loss of oxide single crystals and polycrystalline analogues from 10 to 320 K, J. Eur. Ceram. Soc. 21 (2001) 2605–2611.
[29] S.J. Penn, N.M. Alford, A. Templeton, X.R. Wang, M.S. Xu, M. Reece, K. Schrapel, Effect of porosity and grain size on the microwave dielectric properties of sintered alumina, J. Am. Ceram. Soc. 80 (1997) 1885–1888.
[30] J.D. Breeze, J.M. Perkins, D.W. McComb, N.M. Alford, Do grain boundaries affect microwave dielectric loss in oxides, J. Am. Ceram. Soc. 92 (2009) 671–674.
[31] A.J. Bosman, E.E. Havinga, Temperature dependence of dielectric constants of cubic ionic compounds, Phys. Rev. 129 (1963) 1593–1600.
[32] R.D. Shannon, Dielectric polarizabilities of ions in oxides and fluorides, J. Appl. Phys. 73 (1993) 348–366.
[33] R.D. Shannon, G.R. Rossman, Dielectric constant of $MgAl_2O_4$ spinel and the oxide additivity rule, J. Phys. Chem. Solid. 52 (1991) 1055–1059.
[34] G.H. Rao, K. Bärner, I.D. Brown, Bond-valence analysis on the structural effects in magnetoresistive manganese perovskites, J. Phys. Condens. Matter 10 (1998) L757–L763.
[35] I.D. Brown, K.K. Wu, Empirical parameters for calculating cation-oxygen bond valences, Acta Crystallogr. B 32 (1976) 1957–1959.
[36] I.D. Brown, R.D. Shannon, Empirical bond-strength-bond-length curves for oxides, Acta. Crystallogr. A 29 (1973) 266–282.
[37] E.S. Kim, B.S. Chun, R. Free, R.J. Cernik, Effects of packing fraction and bond valence on microwave dielectric properties of $A^{2+}B^{6+}O_4$ (A^{2+}:Ca, Pb, Ba; B^{6+}:Mo, W) ceramics, J. Eur. Ceram. Soc. 30 (2010) 1731–1736.
[38] D. Liu, S.Y. Zhang, Z. Wu, Lattice energy estimation for inorganic ionic crystals, Inorg. Chem. 42 (2003) 2465–2469.
[39] R. Zurmühlen, J. Petzelt, S. Kamba, V.V. Voitsekhovskii, E. Colla, N. Setter, Dielectric-spectroscopy of $Ba(B'_{1/2}B''_{1/2})O_3$ complex perovskite ceramics-correlations between ionic parameters and microwave dielectric properties. i. infrared reflectivity study (1012-1014Hz), J. Appl. Phys. 77 (199) 5341-5350..
[40] J.C. Kim, M.H. Kim, S. Nahm, J.H. Paik, J.H. Kim, H.J. Lee, Microwave dielectric properties of $Re_3Ga_5O_{12}$ (Re: Nd, Sm, Eu, Dy, and Yb) ceramics and effect of TiO_2 on the microwave dielectric properties of $Sm_3Ga_5O_{12}$ ceramics, J. Eur. Ceram. Soc. 27 (2007) 2865–2870.
[41] D. Liu, S.Y. Zhang, Z. Wu, Lattice energy estimation for inorganic ionic crystals, Inorg. Chem. 42 (2003) 2465–2469.
[42] B.F. Levine, Bond susceptibilities and ionicities in complex crystal structures, J. Chem. Phys. 59 (1973) 1463–1486.
[43] B.F. Levine, A new contribution to the nonlinear optical susceptibility arising from unequal atomic radii, Phys. Rev. Lett. 25 (1970) 440–443.
[44] H.Y. Yang, S.R. Zhang, H.C. Yang, Y. Yuan, E.Z. Li, Intrinsic dielectric properties of columbite $ZnNb_2O_6$ ceramics studied by P-V-L bond theory and infrared spectroscopy, J. Am. Ceram. Soc. 102 (2019) 5365–5374.
[45] H. Yang, S. Zhang, Y. Chen, H. Yang, Y. Yuan, E. Li, Crystal chemistry, Raman spectra, and bond characteristics of trirutile-type $Co_{0.5}Ti_{0.5}TaO_4$ microwave dielectric ceramics, Inorg. Chem. 58 (2019) 968–976.
[46] J. Bao, Y. Zhang, H. Kimura, H. Wu, Z. Yue, Crystal structure, chemical bond characteristics, infrared reflection spectrum, and microwave dielectric properties of $Nd_2(Zr_{1-x}Ti_x)_3(MoO_4)_9$ ceramics, J. Adv. Ceram. 12 (2023) 82–92.